Talanta 277 (2024) 126417

Contents lists available at ScienceDirect

Talanta

journal homepage: www.elsevier.com/locate/talanta

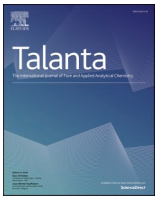

Tracing isotopically labeled selenium nanoparticles in plants via single-particle ICP-mass spectrometry

Bruna Moreira Freire [a,b], Ana Rua-Ibarz [b], Flávio Venâncio Nakadi [b], Eduardo Bolea-Fernandez [b], Juan J. Barriuso-Vargas [c], Camila Neves Lange [a], Maite Aramendía [b], Bruno Lemos Batista [a,**], Martín Resano [b,*]

[a] Federal University of ABC (UFABC), Center for Natural and Human Sciences (CCNH), Santo André, São Paulo, 09210-580, Brazil
[b] University of Zaragoza, Department of Analytical Chemistry, Aragon Institute of Engineering Research (I3A), Zaragoza, 50009, Spain
[c] Universidad de Zaragoza–CITA, AgriFood Institute of Aragon (IA2), Zaragoza, 50059, Spain

ARTICLE INFO

Keywords:
SeNPs
Oryza sativa L.
Single-particle ICP-MS
Biofortification
Foliar exposure
Biotransformation

ABSTRACT

Agronomic biofortification using selenium nanoparticles (SeNPs) shows potential for addressing selenium deficiency but further research on SeNPs-plants interaction is required before it can be effectively used to improve nutritional quality. In this work, single-particle inductively coupled plasma-mass spectrometry (SP-ICP-MS) was used for tracing isotopically labeled SeNPs (^{82}SeNPs) in *Oryza sativa* L. tissues. For this purpose, SeNPs with natural isotopic abundance and ^{82}SeNPs were synthesized by a chemical method. The NPs characterization by transmission electron microscopy (TEM) confirmed that enriched NPs maintained the basic properties of unlabeled NPs, showing spherical shape, monodispersity, and sizes in the nano-range (82.8 ± 6.6 nm and 73.2 ± 4.4 nm for SeNPs and ^{82}SeNPs, respectively). The use of ^{82}SeNPs resulted in an 11-fold enhancement in the detection power for ICP-MS analysis, accompanied by an improvement in the signal-to-background ratio and a reduction of the size limits of detection from 89.9 to 39.9 nm in SP-ICP-MS analysis. This enabled ^{82}SeNPs to be tracked in *O. sativa* L. plants cultivated under foliar application of ^{82}SeNPs. Tracing studies combining SP-ICP-MS and TEM-energy-dispersive X-ray spectroscopy data confirmed the uptake of intact ^{82}SeNPs by rice leaves, with most NPs remaining in the leaves and very few particles translocated to shoots and roots. Translocation of Se from leaves to roots and shoots was found to be lower when applied as NPs compared to selenite application. From the size distributions, as obtained by SP-ICP-MS, it can be concluded that a fraction of the ^{82}SeNPs remained within the same size range as that of the applied NP suspension, while other fraction underwent an agglomeration process in the leaves, as confirmed by TEM images. This illustrates the potential of SP-ICP-MS analysis of isotopically enriched ^{82}SeNPs for tracing NPs in the presence of background elements within complex plant matrices, providing important information about the uptake, accumulation, and biotransformation of SeNPs in rice plants.

1. Introduction

Selenium (Se) is an essential micronutrient for humans and other animals [1,2]. However, it is estimated that approximately 1 billion people worldwide have an insufficient Se intake [3]. Various approaches have been employed to address this issue, including plant biofortification with ionic Se [4] and, more recently, with selenium nanoparticles (SeNPs) [5]. Among the different plants, rice (*Oryza sativa* L.) stands out as a staple food for more people than any other food obtained from a single plant species, being very important for human nutrition [6]. Therefore, increasing the Se content in rice grains through agronomic biofortification is one of the alternatives for addressing Se deficiency [7,8].

In the last years, metal-containing nanoparticles (NPs) have been increasingly used in many fields, including plant science [9,10]. Particularly, the interest in SeNPs has grown as a potential substitute for selenite and selenate in agronomic biofortification of food crops [11–13]. In general, SeNPs are more efficient in the regulation of selenoenzymes, more bioavailable, and less toxic when compared to other organic and inorganic forms of Se [1,14]. Several studies reported that

* Corresponding author.
** Corresponding author.
E-mail addresses: bruno.lemos@ufabc.edu.br (B.L. Batista), mresano@unizar.es (M. Resano).

https://doi.org/10.1016/j.talanta.2024.126417
Received 29 February 2024; Received in revised form 13 May 2024; Accepted 10 June 2024
Available online 12 June 2024

the use of SeNPs shows benefits for plants, including Se biofortification, decrease in metal accumulation, improvement in growth and yield, stimulation of the antioxidant system, and improvement in photosynthesis [15–17].

However, the extensive use of NPs in agriculture generates concerns about crop health and food safety [18]. Further studies are needed to sensitively track SeNPs in plants and determine their behavior and fate in the environment. In this context, inductively coupled plasma-mass spectrometry (ICP-MS), operated in both bulk and single-particle (SP) modes, can provide invaluable information. SP-ICP-MS has emerged as a powerful analytical technique to characterize NPs, as it can simultaneously provide different types of relevant NP information, such as elemental composition, size (spherical equivalent diameter – nm) and size distribution, particle number density (particles/mL) and mass concentration (mg/L) [19,20]. In the last years, SP-ICP-MS has been applied to the characterization of SeNPs in aqueous solutions, as well as in biological tissues [13,21,22].

Tracing SeNPs in complex matrices by SP-ICP-MS is not straightforward. The most abundant Se isotopes – ^{78}Se (23.80 %) and ^{80}Se (49.60 %) – strongly suffer from the occurrence of spectral interferences [23], particularly those from the Ar dimers ($^{38}Ar^{40}Ar^{+}$ and $^{40}Ar_2^{+}$) overlapping at the mass-to-charge (m/z) ratio of $^{78}Se^{+}$ and $^{80}Se^{+}$, respectively. Different strategies have been developed over the years to achieve interference-free conditions, such as the use of collision/reaction cell (CRC) technology in quadrupole-based ICP-MS instrumentation. However, the use of CRC gases may cause loss of sensitivity, hampering the detection of SeNPs [22], while an extension of the NP event duration in SP-ICP-MS, depending on the gas used [24], has also been reported to have a detrimental effect on the characterization of NPs strongly affected by the occurrence of spectral overlap.

Another challenge is the presence of high background elemental contents in complex matrices, such as plant samples, which originate from natural or anthropogenic sources. These conditions, combined with the presence of NPs at low and environmentally relevant concentrations, hamper the sensitive tracking of SeNPs. Furthermore, a recent study provided evidence of the biosynthesis of SeNPs in some plant species [22], which can interfere with the detection of externally applied SeNPs in tracing studies. In this context, the application of isotopically labeled NPs, enriched with stable isotopes, enables the differentiation of NP signals from those of the background, facilitating accurate and precise tracking of these NPs in exposure experiments [25,26]. The combination of isotopic labeling of NPs and SP-ICP-MS improves the detection capabilities of the technique and allows for sensitive tracking of SeNPs in plant samples.

Previous works focused on using SP-ICP-MS for tracing NPs in plant tissues [22,25,27]. However, these studies generally (1) relied on hydroponic experiments, which do not accurately reflect the conditions of rice cultivation, (2) used natural NPs rather than isotopically enriched ones [25], (3) did not specifically investigate SeNPs, and (4) examined NPs absorbed by the roots rather than those absorbed through the leaves.

In this work, isotopically labeled SeNPs (^{82}SeNPs) enriched with the least interfered Se isotope (^{82}Se) were synthesized and used throughout the plant experiments. SP-ICP-MS was used to characterize the synthesized NPs in terms of size and to trace ^{82}SeNPs in plant tissues. To the best of the authors' knowledge, this is the first work to use isotopically enriched SeNPs combined with SP-ICP-MS for tracing studies in complex plant matrices. This study aims to provide further insights into the uptake, accumulation, and biotransformation of SeNPs in *O. sativa* tissues.

2. Experimental section

2.1. Standards, samples, and reagents

Ultra-pure water (resistivity >18.2 MΩ cm) was obtained from a Milli-Q water purification system (Millipore, Molsheim, France). Reagents of analytical purity grade were used for all experiments. For the preparation of samples and standards, nitric acid (HNO_3, 65 % Suprapur®) and hydrochloric acid (HCl, 30 % Suprapur®) were purchased from Merck (Darmstadt, Germany). Hydrogen peroxide (H_2O_2, 30 %, VWR, Belgium) and sodium hydroxide pellets (NaOH, Panreac, Spain) were also used.

Sodium selenite (Na_2SeO_3, Sigma-Aldrich, Germany), polyvinyl alcohol (PVA of molecular weight 70 000, Sigma-Aldrich), and ascorbic acid (Scharlau, Barcelona, Spain) were used to synthesize SeNPs of natural isotopic composition. For the synthesis of isotopically labeled SeNPs (^{82}SeNPs), elemental Se powder (^{82}Se isotope, 99.93 % purity) was purchased from CortecNet (France). Triton X-100 (Merck) was used as a surfactant for NP dilution in plant experiments. Macerozyme R-10 enzyme (pectinase from *Rhizopus* sp., Apollo Scientific, UK), trisodium citrate dihydrate, and citric acid (Merck) were used for NP extraction from plant tissues. Macerozyme R-10 is a multi-component enzyme mixture containing cellulase (0.1 unit per mg), hemicellulase (0.25 unit per mg), and pectinase (0.5 unit per mg).

Single-elemental standard solutions of gold and selenium (1 g L^{-1}, Merck) were appropriately diluted for bulk ICP-MS and SP-ICP-MS analysis. Yttrium and iridium standard solutions (1 g L^{-1}, Merck) were used as internal standards to correct for matrix effects, instrumental drift, and instrument instability for Se and Au determination (bulk ICP-MS), respectively. The reference materials SRM 1568b Rice Flour and SRM 1570a Spinach Leaves from the National Institute of Standards & Technology (NIST, Gaithersburg, MD) were used for QA/QC of the analytical protocol. A NanoXact™ gold nanoparticle (AuNP) suspension of 70 nm nominal diameter (reference diameter: 71 ± 9 nm), obtained from NanoComposix Europe (Prague, Czech Republic), was used in pot experiments. For SP-ICP-MS analysis, the transport efficiency (TE) was determined using AuNPs of 50 nm nominal diameter (reference diameter: 52 ± 5 nm, NanoComposix Europe).

Rice seeds (*O. sativa* ssp. *japonica*) from two varieties (G-Guadiamar and NM-Nuovo Maratelli) were provided by the Instituto Agroalimentario de Aragón-IA2 (Universidad de Zaragoza-CITA). The NM is a tolerant Italian variety, while G is a cold-sensitive variety cultivated in Northeast Spain [28]. An NPK fertilizer (Nitrofoska 15-5-20, EuroChem Agro, Barcelona, Spain) was applied during plant cultivation.

2.2. ICP-MS and SP-ICP-MS parameters and data processing

All the measurements were carried out using a quadrupole-based ICP-MS instrument (NexION 300X, PerkinElmer, Waltham, USA). This instrument is equipped with a quadrupole-based CRC. A quadrupole ion deflector (QID) reflects the ion beam over a 90-degree angle, focusing it into the CRC. The sample introduction system comprises a 0.4 mL min^{-1} concentric quartz nebulizer and a quartz cyclonic spray chamber. In this work, the instrument was operated in no gas or "vented" mode since the monitoring of the ^{82}Se isotope (relative abundance of 8.7 %) is not strongly affected by the occurrence of spectral overlap. The instrumental parameters, such as torch position and sampling depth, were optimized daily following the instructions from the manufacturer. The QID and nebulizer gas flow rates were daily optimized (highest sensitivity for $^{82}Se^{+}$) using a 5 μg L^{-1} ionic standard solution of Se. The liquid flow rate was measured daily by weighing the mass of ultra-pure water taken up by the peristaltic pump during 1 min. The particle size method [20] described by Pace et al. [29] was used to calculate the TE. The ICP-MS instrument settings and data acquisition parameters are gathered in Table 1.

The Syngistix PerkinElmer software with the Nano Application module was used for data acquisition. Raw data obtained using the Syngistix were treated and evaluated externally. For SP-ICP-MS, the so-called Hyper Dimensional Image Processing (HDIP) software was employed to identify and integrate the individual NP events, as described elsewhere [24]. This software was developed at Ghent University for post-processing of spectral data and images in the context of

Table 1
ICP-MS instrument settings and data acquisition parameters.

General conditions	
RF power, W	1500
Plasma gas flow, L min^{-1}	15
Auxiliary gas flow, L min^{-1}	1.2
Nebulizer gas flow, L min^{-1}	1.02 to 1.16
QID, V	−12.7 to −11.0
Nuclides monitored	^{82}Se and ^{197}Au
Bulk analysis parameters	
Internal standards	^{89}Y and ^{193}Ir
Dwell time, ms	10
Sweeps	100
Replicates	10
Integration time, ms	1000
SP-ICP-MS analysis parameters	
Dwell time, μs	100
Acquisition time, s	60
Sample flow rate, mL min^{-1}	0.40-0.53
AuNP density, g cm^{-3}	19.3
SeNP density, g cm^{-3}	4.79
Transport efficiency, %	3.9 to 5.7

laser ablation (LA) ICP-MS and is meanwhile commercially available from Teledyne Cetac Technologies for this purpose, but herein was adopted to identify the individual events appearing randomly during SP-ICP-MS measurements. Subsequently, an Excel (Microsoft, Redmond, USA) spreadsheet composed of two interrelated worksheets was used for calibration and TE calculation and for NP characterization in terms of size distribution, respectively [30]. Such worksheets are a modified version of the ones originally described by Peters et al. [31]. Finally, data was represented using the OriginPro software (version 2021b, 9.85 OriginLab Corporation, Northampton, USA). The size distributions were fitted to Gaussian functions, and their central values were used as mean diameters. A Student *t*-test was used to assess statistical differences between mean diameters at a significance level of 0.05.

2.3. Synthesis of SeNPs and ^{82}SeNPs

SeNPs were synthesized via chemical reduction of Na_2SeO_3 by ascorbic acid, using PVA as a stabilizer. The method used is based on that of Boroumand et al. [32] and Freire et al. [21], with some modifications. Briefly, 10 mL of Na_2SeO_3 12.5 mmol L^{-1} and 10 mL of PVA 0.025 % m/v were mixed. Then, 30 mL of ascorbic acid 12.5 mmol L^{-1} was added dropwise into the mixture (1 mL min^{-1}, Minipuls 3, Gilson, Middleton, USA) under magnetic stirring (HI 190 M, Hanna Instruments, Italy). The color change from uncolored to orange following ascorbic acid addition indicated SeNP formation.

For synthesizing ^{82}SeNPs, selenite was synthesized first using the isotopically enriched ^{82}Se standard [33,34]. For this purpose, 10 mg of ^{82}Se were mixed with 1 mL of concentrated suprapur HNO_3. The mixture was heated at 60 °C in a hotplate (HPX-100, Savillex, MN, USA) for 1 h under argon flow. The resulting solution (~0.2 mL) was made up to 10 mL with ultra-pure water, and the pH was adjusted to 8–9 with NaOH 1 mol L^{-1}. After that, the ^{82}SeNP synthesis was carried out following the same procedure described for SeNPs. The final concentration of Se in the NP suspensions was calculated to be approximately 200 mg L^{-1}.

2.4. Nanoparticle characterization

The synthesized SeNPs and ^{82}SeNPs were characterized by ultraviolet–visible spectrophotometry (UV–vis), transmission electron microscopy (TEM), and SP-ICP-MS. The UV–vis absorption spectra from the solutions obtained in section 2.3 were recorded within the 200–400 nm wavelength range using a UV–vis spectrophotometer (Jasco V-730, USA), after dilution in ultra-pure water. Synthesized NPs were also characterized by TEM to determine the shape, agglomeration state, and size distribution. TEM images were performed in a Tecnai T20 microscope (FEI Company) at a working voltage of 200 kV. Acquired images were evaluated by ImageJ 1.53k software (Wayne Rasband, National Institutes of Health, USA).

For SP-ICP-MS analysis, NP suspensions were stirred and sonicated before dilution. Appropriate dilutions were prepared to minimize the occurrence of double events. The measurement procedure comprised several steps, including the determination of the TE, the calibration using ionic standard solutions of Au (0–3 ng mL^{-1}) and Se (0–20 ng mL^{-1}), and the analysis of the samples, consisting of suspensions of SeNPs and ^{82}SeNPs.

As mentioned before, the TE was calculated by relying on the particle size method, as described elsewhere [29]. After TE calculations, the mass and diameter of each NP in the samples were calculated according to Resano et al. [20].

The size limits of detection (LoD_{size}) were calculated as described by Laborda et al. [35], applying the 3σ criterion for spherical, solid, and pure NPs [36], following Eq. (1):

$$LoD_{size} = \left(\frac{18\sigma_B}{\frac{2}{w}\pi\rho F_P K_{ICPMS} K_M t_{dwell}} \right)^{1/3} \quad \text{Eq.1}$$

where σ_B is the standard deviation of a blank solution measured in SP-ICP-MS mode, w is the peak width when working at microsecond dwell times, ρ is the density of the NPs, F_p is the mass fraction of the element in the NP, K_{ICPMS} is the detection efficiency, K_M is the element factor, and t_{dwell} is the dwell time.

The SP-ICP-MS approach was also used to monitor the long-term stability of the synthesized ^{82}SeNPs upon storage. For this purpose, the suspension of synthesized NPs was stored at 4 °C and the stability was evaluated after 5 months.

2.5. Plant cultivation and exposure assay

To trace the uptake, accumulation, and biotransformation of SeNPs by plants, the experimental design was set up as a completely randomized 4 x 2 factorial scheme, with 4 treatment groups (control, ^{82}SeNPs, sodium selenite, and AuNPs) and two seed varieties (G and NM).

The rice seeds were germinated in water for 10 days, and subsequently, the viable seeds were transferred to 0.5 L pots containing a mixture of topsoil, organic matter, and sand in a 1.5:1.5:1 ratio [37]. Each group consisted of four pots with 6 seeds per pot, except for AuNPs (two pots). Plants were cultivated under greenhouse conditions from April to September 2023 at the Polytechnic School of Huesca (University of Zaragoza, Spain). The water regime was flooding, with 3–4 cm of water after 15 days. On day 30, plants were fertilized with NPK 15-5-20, which was distributed equally in all pots according to the manufacturer's instructions.

Thirty-day-old plants were exposed to isotopically labeled ^{82}SeNPs, AuNPs, or Se salt by foliar spraying. The Se concentration applied was 10 mg L^{-1} in the groups of ^{82}SeNPs and sodium selenite, based on a previous study that recommended this concentration of sodium selenite as appropriate for foliar rice fertilization [38]. A suspension of 70 nm AuNPs was applied in the AuNP group (at 1 mg L^{-1}). Triton X-100 0.1 % m/v was used as a surfactant in all dilutions. Plants of each group were sprayed in the morning (from 8:00 to 10:00h) until the solution was uniformly distributed on the leaves' surface. A total of four applications were made, with an interval of three days between each application, except for the AuNP group, in which only two applications were made.

At the end of the vegetative period (approximately 45 days), the plants of three pots per group were harvested (one pot for the AuNP group). The roots, shoots, and leaves were separated, washed individually with tap water, rinsed with ultra-pure water 5 times, and oven-dried (50 °C) until constant weight. Then, the rice tissues were roughly cut into small pieces with metal-free scissors and stored until sample preparation. At this point, the plants of one pot per group were

transplanted to 3.4 L pots and cultivated until grain maturation, with two more foliar applications starting at the flowering stage. After complete maturity, the grains were harvested and oven-dried (50 °C) until constant weight. Then, husks were removed, and the grains were ground manually with a ceramic mortar and pestle and stored until sample preparation as described below.

2.6. Tracing nanoparticles in rice plants

2.6.1. Acid digestion for bulk ICP-MS analyses

Samples were acid-digested and bulk-analyzed by ICP-MS to study the uptake and accumulation of NPs by rice plants. A fraction of 0.025 g of dried and homogenized sample was accurately weighed in Savillex PFA beakers, and 2 mL of 14 M HNO_3 were added. After 24 h of pre-digestion at room temperature, 0.7 mL of H_2O_2 (30 %) was added, and samples were digested on a hot plate at 110 °C for 7 h. Subsequently, the solutions were evaporated at 70 °C until almost dryness. Finally, the residue of each sample was diluted to 2 mL using 0.7 M HNO_3 for the reference materials, control samples, and samples treated with ionic Se and SeNPs, and 0.6 M HCl for the samples treated with AuNPs. Digestions were made in triplicate. Prior to ICP-MS analysis, the sample digests were diluted for appropriate quantification via external calibration (concentrations ranging from 0 to 10 μg L^{-1} for Au and from 0 to 25 μg L^{-1} for Se). The limits of detection (LoDs) and of quantification (LoQs) were calculated as 3 and 10 times the standard deviation of 10 consecutive measurements of a blank solution, divided by the slope of the calibration curve, respectively. Significant differences between groups (at a 95 % significance level; $p = 0.05$) were evaluated by one-way analysis of variance (ANOVA). Two standard reference materials (NIST 1568b Rice Flour and NIST 1570a Spinach Leaves) were subjected to the same procedure for QA/QC ($n = 3$) of the analytical protocol. A recovery ranging between 106 and 120 % was achieved.

2.6.2. Enzymatic digestion for SP-ICP-MS analyses

To assess the biotransformation and size distributions of NPs in rice tissues, plant samples were digested with Macerozyme R-10, according to the procedure reported by Jiménez-Lamana et al. [27], with minor modification. The procedure consisted of two steps: homogenization of the sample with citrate buffer and incubation with enzyme solution in a water bath [27]. In this study, the mixture was homogenized in an ultrasonic bath (USC200T, VWR International; 45 kHz and 60 W, Amsterdam, the Netherlands) rather than in an ultrasonic probe, as previously reported by Jiménez-Lamana et al. [27]. The sonication time was optimized from 0 to 120 min to extract the highest number of NPs without affecting the NP size distribution (cf. Section 3.3). The initial optimization was carried out using a 70 nm AuNPs commercial suspension and rice leaves from the group exposed to AuNPs (NM variety) since sizing AuNPs by SP-ICP-MS is more straightforward. Enzyme-digested samples were directly analyzed by SP-ICP-MS without further dilution. Digestions were performed per duplicate, and blanks were analyzed throughout the experiment. To assess a possible effect of the enzymatic digestion on the ^{82}SeNPs, the synthesized suspension was subjected to the same procedure and analyzed by SP-ICP-MS, after 50-fold dilution with ultra-pure water.

2.6.3. TEM and EDS

The NPs extracted from rice leaves by the enzymatic procedure were also characterized by TEM. TEM images were performed in a Tecnai F30 high-resolution (HR) microscope (FEI Company) at a working voltage of 300 kV. The microscope is equipped with an energy-dispersive X-ray spectroscopy (EDS) system, allowing for confirmation of the NPs elemental composition.

3. Results and discussion

3.1. Characterization of SeNPs and ^{82}SeNPs

The accurate characterization of NPs in terms of size, size distribution, and morphology relies on the combination of the results obtained via multiple analytical techniques [9]. In this work, UV–vis, TEM, and SP-ICP-MS were used to characterize the synthesized NPs. The SeNPs and ^{82}SeNPs were characterized via UV–vis absorption spectrometry within the 200–400 nm range. The presence of an absorption peak at 265 nm (Fig. S1), indicative of surface plasmon resonance excitation, confirmed the formation of SeNPs in both suspensions; this peak results from the reduction of selenite to SeNPs [21,39,40]. TEM analysis showed that both SeNPs and ^{82}SeNPs are monodisperse (RSD <10 %) and spherical, with sizes of 82.8 ± 6.6 and 73.2 ± 4.4 nm, respectively (Fig. S2). The smaller average size of the isotopically enriched ^{82}SeNPs can be attributed to the nucleation and growth processes of the NPs, which are influenced by the relative concentrations of the reducing agent and the precursor [41]. For a detailed discussion on the UV-vis and TEM characterization of SeNPs and ^{82}SeNPs, please refer to the supplementary information.

In addition to UV–vis and TEM analysis, the NP suspensions were also characterized via SP-ICP-MS by relying on the monitoring of the less interfered ^{82}Se nuclide (natural abundance = 8.73 %). Fig. 1A and B shows the time scans obtained for SeNPs and ^{82}SeNPs, respectively.

As can be seen in Fig. 1A, it was not possible to distinguish between the signal events generated by natural SeNPs and the background signal under the selected measurement conditions. To overcome this limitation, the synthesis of isotopically enriched ^{82}SeNPs allowed for an improvement in the signal-to-background ratio (approx. 11-fold). Fig. 1B shows that the ^{82}SeNP events could easily be distinguished from the background signal. Data processing showed that the average integrated intensity of ^{82}SeNPs was 27.03 counts. Considering the natural abundance of ^{82}Se, this signal intensity would be 2.36 counts for natural SeNPs, which in practice makes it impossible to distinguish the NP signal using the ^{82}Se nuclide for signal monitoring. In addition, the theoretical LoD_{size} determined according to Eq. (1) was lowered to less than half, from 89.9 for SeNPs to 39.9 for ^{82}SeNPs. Nath et al. also reported that using isotopically labeled metallic NPs for tracing studies in plants improved detection capabilities [25]. Therefore, the method was found to be suitable for characterizing the synthesized ^{82}SeNPs (TEM = 73.2 ± 4.4 nm), as shown in Fig. 2A. The average diameter obtained was 74.1 ± 7.8 nm, which was found to be in excellent agreement with the TEM results ($p > 0.05$).

The stability of the synthesized NPs is an important parameter to be studied when samples may be stored before analysis [40]. The particle size distribution obtained after 5 months (Fig. 2B, red bars, mean diameter = 77.4 ± 7.3 nm) showed no significant difference ($p > 0.05$) compared to freshly synthesized NPs (Fig. 2B, blue bars, mean diameter = 74.1 ± 7.8 nm). Therefore, the ^{82}SeNPs were considered stable for more than 5 months. The use of PVA as stabilizer can be related to the observed stability.

3.2. Gold and selenium accumulation in rice tissues from different varieties

The total Au content was determined in acid-digested roots (25.4 ± 4.2 μg kg^{-1}), shoots (40.5 ± 15 μg kg^{-1}), and leaves (429 ± 74 μg kg^{-1}) of plants from NM variety exposed to 70 nm AuNPs aiming to identify the tissue type with the highest Au accumulation. Even though investigating the behavior of AuNPs is not the topic of the current study, this was performed in order to use this tissue for optimization of the enzymatic digestion protocol (cf. Section 3.3). The results indicate that rice plants can uptake Au when applied as AuNPs on the leaves. The Au accumulation followed the order: leaves > shoots > roots. Based on these results, leaves from the AuNP exposed group were used for the

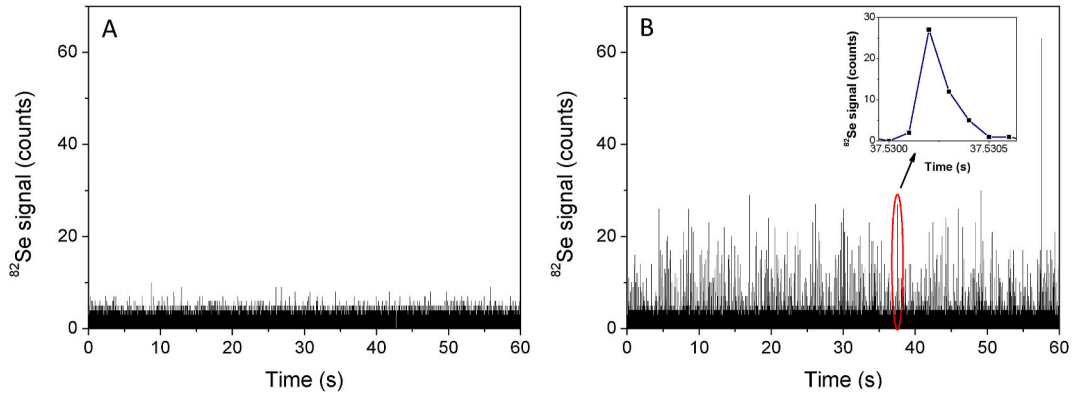

Fig. 1. $^{82}Se^{+}$ time scans obtained for (A) SeNP and (B) ^{82}SeNP suspensions. The inset in Fig. (B) shows an example of the peak shape obtained for an individual NP.

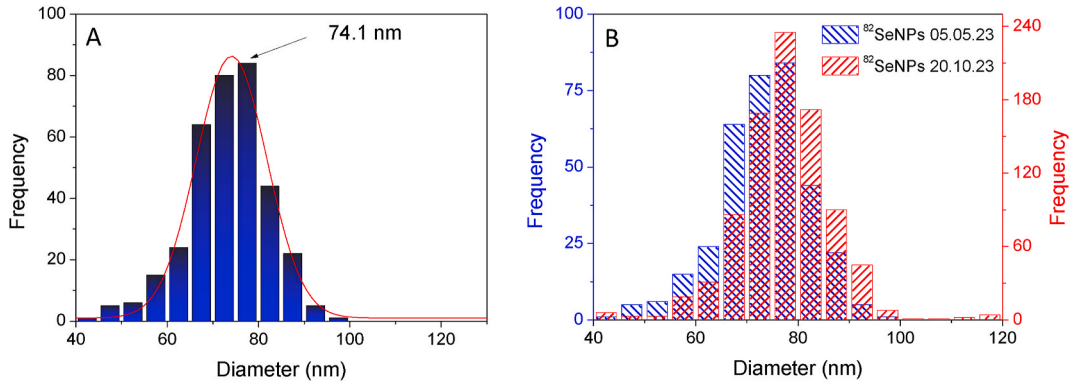

Fig. 2. (A) Particle size distribution of ^{82}SeNP suspensions obtained by SP-ICP-MS. The mean diameter was 74.1 ± 7.8 nm (mean ± s). (B) Effect of storage time on the stability of ^{82}SeNPs. Size distributions obtained by SP-ICP-MS for the fresh suspension (blue) and the same suspension after five months of storage at 4 °C (red). The diameters were 74.1 ± 7.8 nm and 77.4 ± 7.3 nm (mean ± s), respectively.

enzymatic digestion optimization, as described in section 3.3.

The total Se content was determined in rice roots, shoots, leaves, and grains from the two *O. sativa* varieties (NM and G). Control, Na_2SeO_3, and ^{82}SeNP-treated plants were analyzed. The calibration data and instrumental (bulk) LoDs and LoQs for natural and isotopically enriched Se standards are shown in Table 2. The use of ^{82}Se-enriched standards allowed for an 11-fold increase in detection capabilities, as indicated before.

The results of plant analysis are presented in Table 3. For the Na_2SeO_3 and ^{82}SeNPs-treated plants, the highest amount of Se was found in leaves, followed by shoots, for both rice varieties. Comparing the treatments, the application of Na_2SeO_3 caused a greater increase in Se concentrations in rice roots, shoots, and grains, while the Se content in leaves was similar (no statistical difference detected) between Na_2SeO_3 and ^{82}SeNPs groups. This suggests that the uptake behavior of Se by *O. sativa* leaves is quite similar independently of the application in ionic or nanoparticulate form. However, the use of ionic Se results in a greater translocation to other plant parts. The rice grains of the Na_2SeO_3 treated group presented significantly higher (2- and 4-fold) Se concentrations than the grains of the ^{82}SeNPs treated group for NM and G varieties, respectively. It has already been demonstrated that foliar application of sodium selenite effectively increased the accumulation of Se in rice grains [7,38]. Wang et al. demonstrated with hydroponic experiments that SeNPs can be absorbed by rice roots, however, the uptake

Table 2
Comparison of calibration data and instrumental limits of detection (LoDs) and of quantification (LoQs), obtained for $m/z = 82$ determination using ICP-MS in standards with natural isotopic composition of Se and standards enriched with ^{82}Se. LoDs and LoQs were calculated as 3 and 10 times the standard deviation on 10 consecutive measurements of a blank solution, divided by the slope of the calibration curve, respectively.

Parameter	Natural Se abundance	^{82}Se-enriched standards
Sensitivity (cps L μg^{-1})	1066	12201
R^2	0.999991	0.999991
LoD (μg L^{-1})	0.27	0.024
LoQ (μg L^{-1})	0.92	0.080

Table 3
Total Se content in different tissues of two rice varieties (NM- Nuovo Maratelli and G- Guadiamar) from control, sodium selenite, and ^{82}SeNP treated plants (average ± standard deviation, n = 3).

Se concentration (mg kg^{-1})	Rice variety	Roots	Shoots	Leaves	Grains
Control-plants	NM	<LoQ	<LoQ	0.58 ± 0.005*^{a}	<LoQ
	G	<LoQ	<LoQ	0.39 ± 0.18^{a}	<LoQ
Na_2SeO_3-treated plants	NM	1.05 ± 0.18^{a}	3.87 ± 0.44^{ab}	13.9 ± 1.4^{b}	0.63 ± 0.04^{a}
	G	1.74 ± 0.15^{b}	6.15 ± 1.12^{a}	18.2 ± 2.9^{b}	1.30 ± 0.03^{b}
^{82}SeNP-treated plants	NM	0.29 ± 0.04^{c}	2.20 ± 0.67^{b}	15.8 ± 3.9^{b}	0.30 ± 0.001^{c}
	G	0.60 ± 0.10^{c}	3.60 ± 1.16^{b}	19.1 ± 2.9^{b}	0.31 ± 0.01^{c}

* From the three analyzed biological replicates, Se was quantified just in one, while the other two were below the LoQ. In this case, the standard deviation reflects the instrumental measurement repeatability. A one-way ANOVA was carried out and the results are also shown: different superscript letters denote a significant difference ($p < 0.05$) between groups for the same column (e.g., within each column, "a" is similar to "a" and different from "b", etc.).

rate was found to be lower than that of selenite [42]. A recent study has demonstrated that, when SeNPs are sprayed onto plant leaves, Se is transported both upwards and downwards in the plant [13]. Selenium translocation to other plant parts (roots, shoots, and grains), when applied in the nanoparticulate form, was also observed in this work, despite having a lower translocation rate compared to selenite, confirming that agronomic biofortification with Se can be carried out by foliar application of either selenite or SeNPs.

Self-evidently, different Se formulations exhibit differences in toxicity and bioavailability that are crucial for biofortification programs and for ensuring food safety, given the narrow range between normal and toxic Se levels [43]. However, the underlying reasons for these differences are not yet fully understood. Some studies have shown that SeNPs are more bioavailable than both organic and inorganic forms of Se [44,45]. Conversely, Hadrup and Ravn-Haren reported that the bioavailability of Se compounds follows the ascending order: nanoparticulate Se < selenite < organic Se [46]. The lower toxicity of SeNPs compared to other forms of Se is well documented [44,45].

Comparing the rice varieties subjected to the same treatment, it was observed that, for roots and grains, the G variety accumulated significantly more Se than the NM for the Na_2SeO_3-treated plants. These results suggest that the G variety can be a natural Se accumulator, and then its use in Se biofortification programs may be more suitable. It is known that different rice varieties can accumulate nutrients and potentially toxic elements differently [47]. From the results reported in this work, it can be concluded that Se accumulation in rice plants is influenced by its physicochemical form and the bioaccumulation mechanism of the plant variety.

3.3. Optimization of the enzymatic digestion method

Studies reporting enzymatic digestion of plant tissues typically involve tissue homogenization using an ultrasonic probe [25,27] or even a tissue ruptor [22]. In this work, the procedure developed by Jiménez-Lamana et al. [27] was used, but a common ultrasonic bath was employed for tissue homogenization. The sonication time during the homogenization was optimized from 0 to 120 min, while the extraction yield and size distributions of AuNPs were monitored (Supplementary Fig. S3).

As shown in Fig. S3A and a trend of increase in digestion efficiency with increasing sonication times during the homogenization was observed. More than 120 min of sonication was not assessed due to the heating of the samples and to avoid making the procedure more time-consuming.

The effect of sonication time on the NP size distribution was investigated for both the AuNP suspension and the NPs extracted from rice leaves (Fig. S3B). The results showed similar size distributions for AuNPs extracted from rice leaves using all the tested sonication times. Moreover, for all sonication times, the mean diameter obtained for extracted particles was in good agreement with that obtained for the original suspension of AuNPs. Figs. S3C and S3D show that the size distributions obtained after the enzymatic procedure using 120 min of sonication for the 70 nm AuNP stock suspension (64.3 ± 11.1 nm) and for the AuNPs extracted from rice leaves (68.1 ± 11.0 nm) were in good agreement. Therefore, it can be concluded that the use of an ultrasonic bath is suitable for extracting AuNPs from rice tissues without causing particle dissolution or significant agglomeration.

Sonication times ranging from 0 to 120 min were also tested for the extraction of ^{82}SeNPs from rice leaves of the NM variety. Fig. 3A shows that, as observed for AuNPs, increasing the sonication time increased the efficiency of ^{82}SeNP extraction.

The effect of the digestion procedure on the stability of ^{82}SeNPs was also evaluated. For this purpose, the optimum conditions were applied to a suspension of ^{82}SeNPs, and the mean diameters obtained before and after the digestion procedure (Fig. 3B) showed no statistical difference at the 95 % significance level ($p > 0.05$). Therefore, the results confirmed that neither the digestion process nor the matrix of the extraction enzyme affected the NP size distribution. Based on these results, 120 min of sonication was chosen as the optimal condition for the following experiments.

A high dispersion in the number of particles was observed in Fig. S3A and Fig. 3A, mainly for high sonication times. Despite compromising the accurate quantification of SeNPs by SP-ICP-MS, this dispersion expresses the natural plant-to-plant variability that is characteristic of crop plants [48], since data corresponds to biological replicates. The high standard deviation may also indicate a limitation of the digestion procedure since it increased with increasing sonication times. Plant samples are complex matrices, and the determination of particle-based concentration and mass concentration is a challenge due to non-spectral interferences caused by the matrix. Recently, the feasibility of SP-ICP-MS for the characterization and quantification of AgNPs in a plant cell medium culture was demonstrated by da Silva and Arruda [49]. The authors observed signal suppression at high cell medium culture concentration, hampering the accurate determination of the mass-based concentration. A matrix-matching calibration was performed to overcome these interferences [49]. Other strategies to handle the matrix effects are based on using a higher dilution factor when the number of particles is high, internal standardization, and standard addition [49–51]. Similarly to the cell medium culture, the high content of salts and organic compounds in plant enzymatic extracts can cause a critical matrix effect. However, the determination of the particle-based concentration is considered beyond the scope of this work, as our focus was to develop a

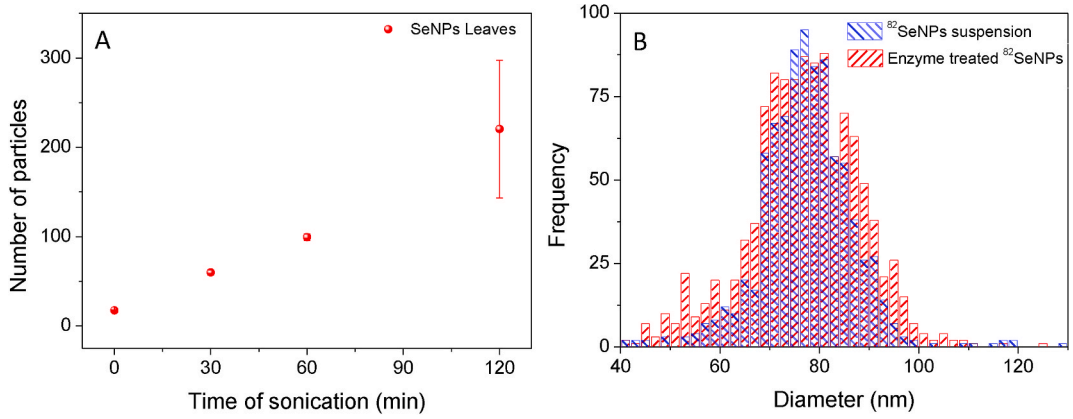

Fig. 3. (A) Number of events of ^{82}SeNPs extracted from rice leaves by enzymatic digestion (n = 2), with increasing sonication times. The uncertainties are expressed as standard deviation. (B) Size distributions obtained for ^{82}SeNPs suspension before (blue) and after (red) enzymatic digestion. The diameters were 77.7 ± 7.4 and 77.9 ± 9.8 nm (mean ± s), respectively.

methodology for the detection and size-characterization of isotopically enriched ^{82}SeNPs for tracing experiments in plant tissues.

3.4. Tracing ^{82}SeNPs in rice tissues by SP-ICP-MS

The calculations performed to obtain the size distribution by SP-ICP-MS involve assuming that the NPs are spherical and that they are pure metallic SeNPs. Therefore, the use of complementary techniques (such as TEM) to confirm the sphericity and chemical composition of NPs extracted from plant tissues is highly recommended. For this purpose, the enzymatic extracts of rice leaves from NM and G varieties exposed to ^{82}SeNPs were analyzed by TEM-EDS. The results are shown in Supplementary Figs. S4A and S4B for the NM and G varieties, respectively. TEM images showed the presence of sphere-shaped NPs with diameters of approximately 100 nm. EDS spectra showed the presence of a strong peak at 1.5 keV, which is characteristic of Se [52], confirming that the NPs are mainly composed of this element. Size histograms could not be obtained due to the low particle concentration in the extracts. Still, the presence of spherical SeNPs in exposed rice leaves can be confirmed based on these results.

Before the analysis of ^{82}SeNP-treated samples, the control and Na_2SeO_3-treated samples were enzymatically digested and analyzed by SP-ICP-MS. The time scans obtained for representative samples of each tissue and group, as well as those obtained for blank solutions, are provided in the Supplementary Figs. S5–S6 and in Figs. 4 and 5.

For control samples, no NP events were identified in roots, shoots, and leaves for both rice varieties, and time scans were comparable to those obtained for blanks (Figs. S5 and S6). A similar trend was observed for Na_2SeO_3-treated samples (Fig. 4A, B, and C; and Fig. 5A, B, and C). However, for this group, an increase in the baseline intensity was

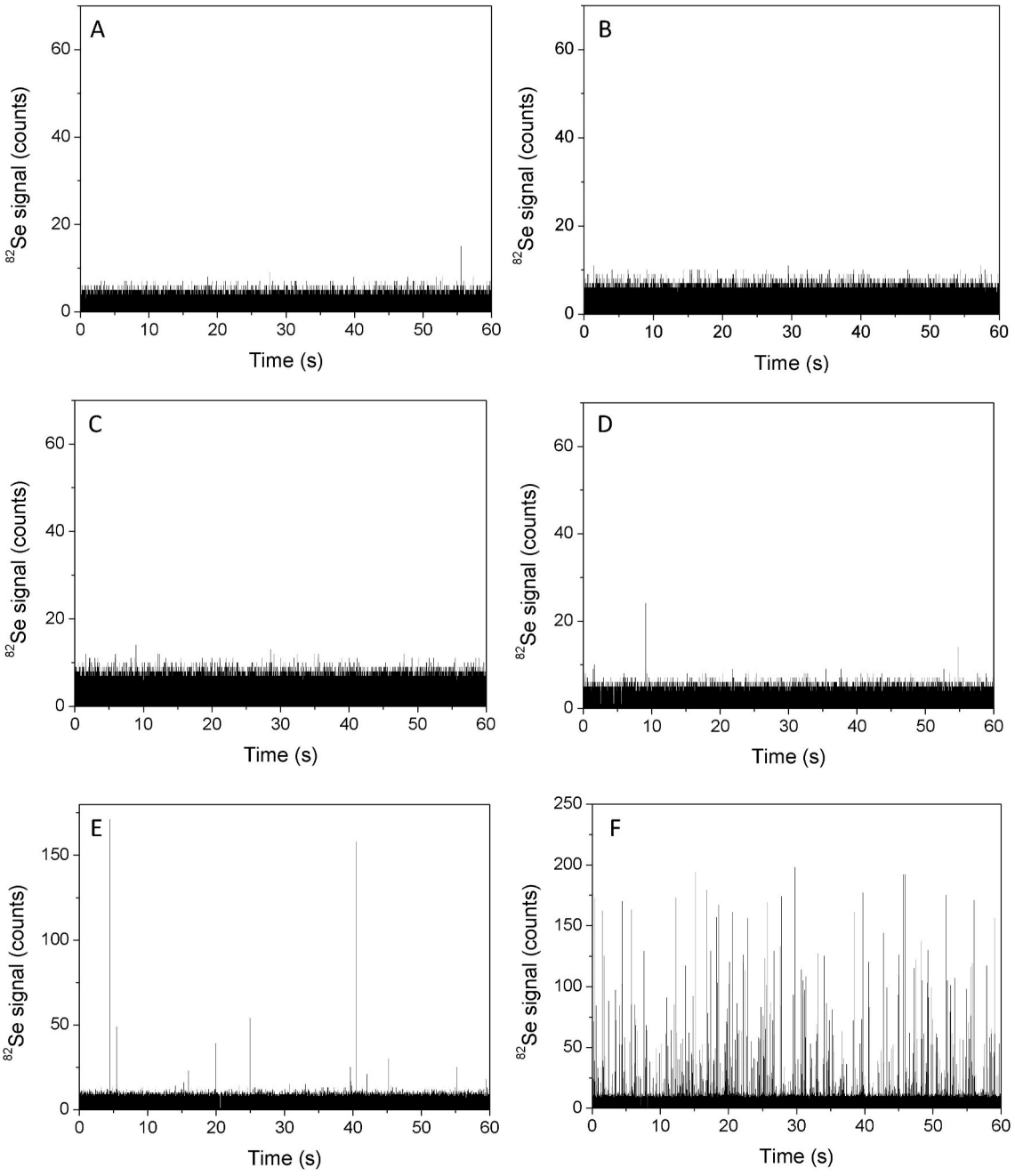

Fig. 4. ^{82}Se time scans obtained for Na_2SeO_3-treated samples of rice (A) roots, (B) shoots, and (C) leaves, and for ^{82}SeNPs-treated samples of (D) roots, (E) shoots, and (F) leaves from Nuovo Maratelli variety, after enzymatic digestion procedure.

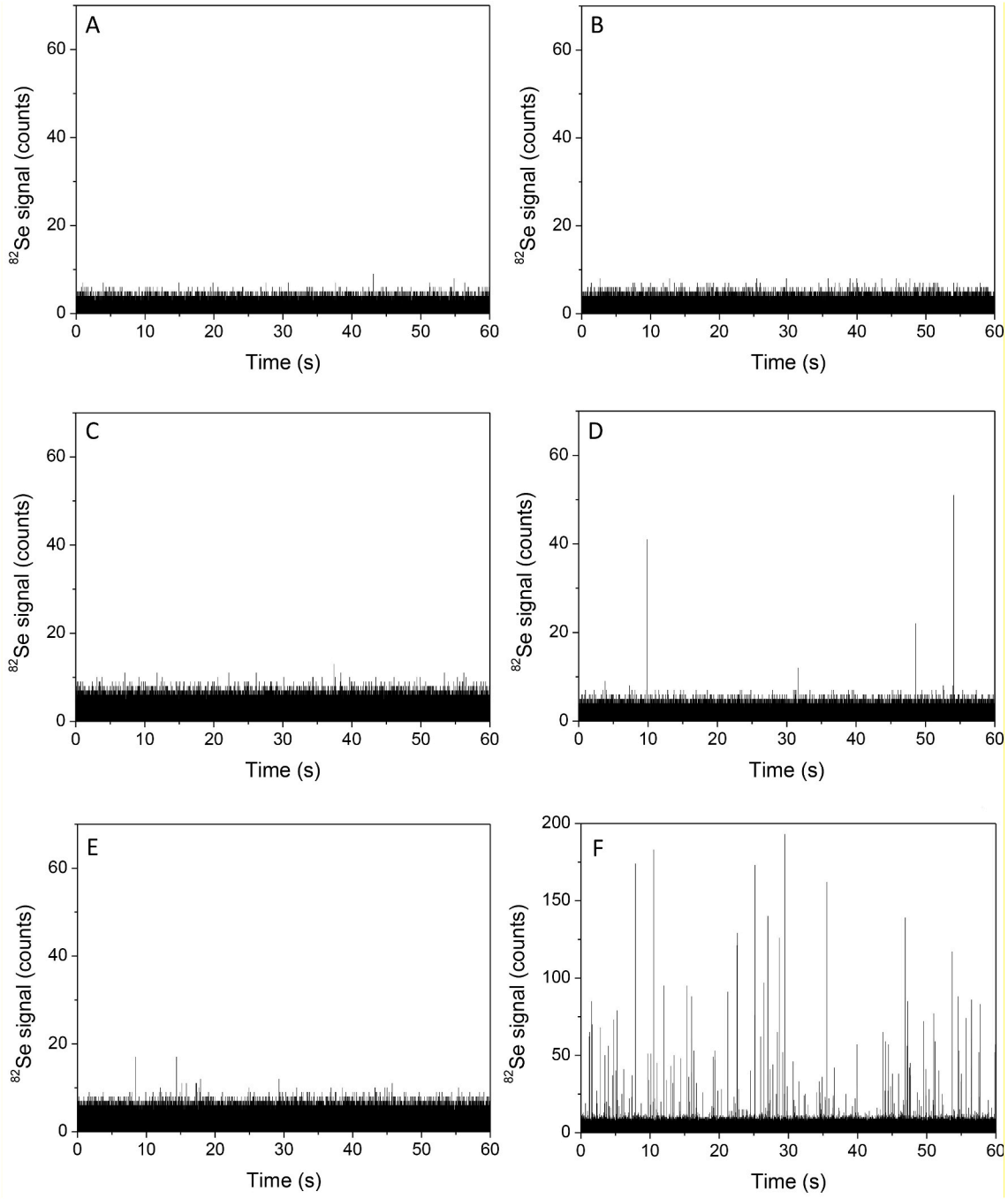

Fig. 5. ^{82}Se time scans obtained for Na_2SeO_3-treated samples of rice (A) roots, (B) shoots, and (C) leaves, and for ^{82}SeNPs-treated samples of (D) roots, (E) shoots, and (F) leaves from Guadiamar variety, after enzymatic digestion procedure.

observed following the ranking: roots < shoots < leaves. This can be explained by the ionic Se concentration, which increased in the same ascending order. Although some plants can be able to biosynthesize SeNPs when exposed to sodium selenite [22], no SeNPs were detected in this work for plants treated with Na_2SeO_3. This can be explained by the low sensitivity of the method to detect natural SeNPs via the monitoring of the ^{82}Se nuclide or by the high background signal resulting from ionic Se. Still, considering the LoD_{size} obtained, it is possible to discard the presence of natural SeNPs larger than 89.9 nm.

The optimized method was then applied for the sensitive tracing of ^{82}SeNPs present in rice roots, shoots, and leaves of the group exposed to ^{82}SeNPs. A clear trend was observed between plant tissues regarding the detection of NPs (Fig. 4D, E, and F; and Fig. 5D, E, and F). For both varieties, none or very few particles were identified in roots and shoots, which was not enough to obtain a size distribution. However, from 375 to 804 signal events were detected on the leaves, which was found to be in good agreement with the total Se determination (section 3.2) and the higher accumulation in the leaves. Moreover, an increase in the baseline was observed for tissues of groups exposed to ^{82}SeNPs as compared to control samples, mainly for leaves and shoots, suggesting that a fraction of the NPs was solubilized and oxidized to ionic Se during the uptake and translocation processes in rice plants. The results confirmed that *O. sativa* absorbed ^{82}SeNPs by leaves' stomata, with a fraction of the Se remaining in the form of NPs on the leaves and very few NPs transported as such downwards in the plant. Another possibility is that ionic Se from ^{82}SeNPs dissolution is accumulated in the leaves and transported to the

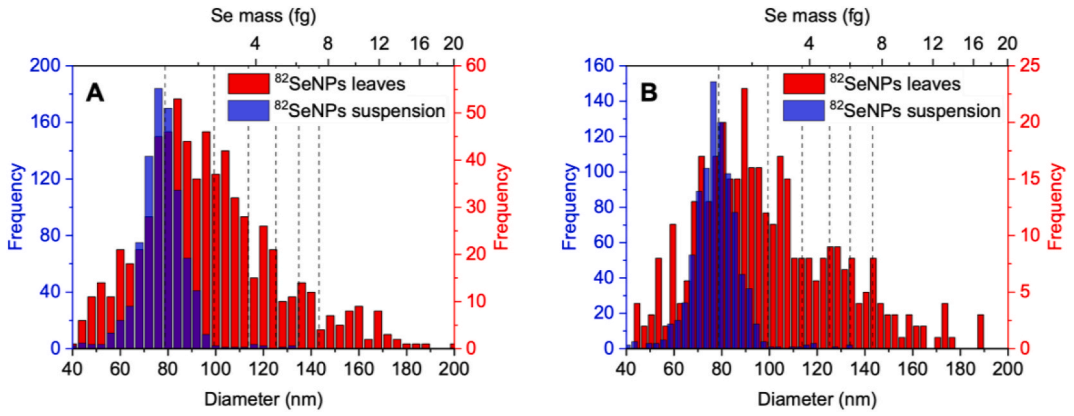

Fig. 6. Size distribution (primary x-axis) obtained for ^{82}SeNP suspension (blue) and for ^{82}SeNPs extracted from rice leaves by enzymatic digestion for varieties NM (A) and G (B). The vertical dashed lines (top x-axis) represent the mass (fg) equivalent to a single ^{82}SeNP or aggregates of multiple ^{82}SeNPs of 2–6 units.

shoots and roots where the *in vivo* formation of SeNPs may occur, as reported by Verstegen and Günther [22].

The size distributions could be obtained for ^{82}SeNPs extracted from the leaves of the NM and G varieties and the results were compared with the original ^{82}SeNP distribution (Fig. 6A and B, respectively). The size histograms obtained for both varieties presented very similar distribution patterns, with a broad size distribution compared with the ^{82}SeNP original size distribution. The first particle distribution is in the same size range as the original ^{82}SeNP suspension, with the most frequent detected sizes ranging between 70 and 90 nm, consistent with the results obtained by TEM. These results confirm that *O. sativa* can uptake intact ^{82}SeNPs. On the other hand, a second distribution at higher sizes (up to 200 nm) was also observed. This broadening of the size distribution can be attributed to the occurrence of multiple events, suggesting that ^{82}SeNPs probably went through an agglomeration process in rice leaves. Nanoparticle agglomeration was confirmed by HR-TEM. Figs. S7A and B show agglomerates of two or more particles in enzyme-digested rice leaves. The agglomeration process of metallic NPs in plants is not fully understood. Jiménez-Lamana et al. observed that PtNPs agglomerated in *Lepidium sativum* and *Sinapis alba* plants [27]. The authors attributed the agglomeration process to mutual attraction between NPs via chemical bonds or van der Waals forces. The NP chemical composition and the plant species may affect the formation of these aggregates [27]. This explains why no agglomeration was observed when rice plants were treated with AuNPs, as shown in Fig. S3D. No significant differences were observed in the biotransformation mechanisms of ^{82}SeNPs between NM and G varieties.

The SP-ICP-MS results obtained using the sensitive method developed for tracing isotopically labeled SeNPs confirmed the internalization of nanoparticulate Se by rice leaves and provided further insights into the accumulation, translocation, and biotransformation of these NPs in plant systems. This knowledge about NP-plant interactions is relevant because there is still no legislation for the use of NPs in agriculture or the remediation of these NPs in the environment [9]. Also, the potential ecological or health impacts of these materials need to be considered. Once released in the agricultural systems, NPs undergo transformations [53]. The partial dissolution of NPs, as evidenced by the results of this study, may produce more available forms of Se and alter toxicity [54]. The biotransformation of SeNPs into selenite and organo-selenium in plants was reported before [13,42]. Nevertheless, the persistence of a fraction of Se in nanoparticulate form and the possible bioaccumulation and human consumption are concerns that still need to be clarified. There are several reviews on the applications, fate, bioaccumulation, and toxicity of NPs [53,55,56], but the impact of nanomaterials on the environment and human health is still not fully understood.

4. Conclusion

The use of isotopically labeled ^{82}SeNPs combined with SP-ICP-MS enhanced the detection capabilities and allowed for the sensitive tracing of ^{82}SeNPs extracted from rice tissues. Tracing studies of total Se content in *O. sativa* by ICP-MS revealed that the application of both ^{82}SeNPs and sodium selenite had the potential to produce rice grains with increased Se content. Se concentration and translocation in rice tissues were significantly affected by Se forms and rice variety.

The SP-ICP-MS results confirmed the uptake of intact ^{82}SeNPs by rice leaves. Moreover, size distributions obtained by SP-ICP-MS indicated that ^{82}SeNPs underwent an agglomeration process in the leaves, while very few NPs were found in shoots and roots following foliar application. HR-TEM-EDS analysis of enzymatic digested leaves confirmed the uptake of spherical NPs composed of elemental Se, and the agglomeration processes occurring in rice leaves. This comprehensive study design with isotopically labeled ^{82}SeNPs brings further insights on NP-plant interactions, improving our understanding of the uptake, accumulation, translocation, and biotransformation of SeNPs in rice plants, which is essential for their application in biofortification programs and for risk assessment. The related mechanisms are outside the scope of this work and need to be further elucidated.

CRediT authorship contribution statement

Bruna Moreira Freire: Writing – review & editing, Writing – original draft, Visualization, Validation, Investigation, Formal analysis, Data curation, Conceptualization. **Ana Rua-Ibarz:** Writing – review & editing, Supervision, Project administration, Conceptualization. **Flávio Venâncio Nakadi:** Writing – review & editing, Visualization, Supervision, Methodology. **Eduardo Bolea-Fernandez:** Writing – review & editing, Supervision, Conceptualization. **Juan J. Barriuso-Vargas:** Writing – review & editing, Supervision, Resources, Methodology, Conceptualization. **Camila Neves Lange:** Writing – review & editing, Supervision, Methodology, Conceptualization. **Maite Aramendía:** Writing – review & editing, Supervision, Project administration. **Bruno Lemos Batista:** Writing – review & editing, Supervision, Resources, Project administration, Funding acquisition, Conceptualization. **Martín Resano:** Writing – review & editing, Supervision, Resources, Project administration, Funding acquisition, Conceptualization.

Declaration of competing interest

The authors declare that they have no known competing financial interests or personal relationships that could have appeared to influence the work reported in this paper.

Data availability

Data will be made available through Zenodo, upon acceptance

Acknowledgments

This work was supported by the São Paulo Research Foundation (FAPESP, grants #2020/00284-2 and 2022/04254-6), the project PID2021-122455NB-I00 (funded by MCIN/AEI/10.13039/501100011033/and ERDF A way of making Europe), the Aragon Government (Construyendo Europa desde Aragón, Group E43_20R). This study was financed in part by the Coordenação de Aperfeiçoamento de Pessoal de Nível Superior - Brasil (CAPES) - Finance Code 001. Ana Rua-Ibarz thanks the European Union's Horizon 2020 research and innovation program under the Marie Sklodowska-Curie grant agreement No 101034288. Eduardo Bolea-Fernandez acknowledges financial support from the Ramón y Cajal programme (RYC2021-031093-I) funded by MCIN/AEI/10.13039/501100011033 and the European Union (NextGenerationEU/PRTR). The authors would like to acknowledge the use of Servicio General de Apoyo a la Investigación-SAI, Universidad de Zaragoza.

Appendix A. Supplementary data

Supplementary data to this article can be found online at https://doi.org/10.1016/j.talanta.2024.126417.

References

[1] K. Badgar, The synthesis of selenium nanoparticle (SeNPs)–Review, Acta agrar, Debr. 1 (2019) 5–8, https://doi.org/10.34101/actaagrar/1/2359.
[2] A.R. dos Reis, H. El-Ramady, E.F. Santos, P.L. Gratão, L. Schomburg, Overview of selenium deficiency and toxicity worldwide: affected areas, selenium-related health issues, and case studies, in: E.A.H. Pilon-Smits, L.H.E. Winkel, Z.Q. Lin (Eds.), Selenium in Plants: Molecular, Physiological, Ecological and Evolutionary Aspects, Springer, Cham, Switzerland, 2017, pp. 209–230.
[3] G.D. Jones, B. Droz, P. Greve, P. Gottschalk, D. Poffet, S.P. McGrath, S. I. Seneviratne, P. Smith, L.H. Winkel, Selenium deficiency risk predicted to increase under future climate change, Proc. Natl. Acad. Sci. 114 (2017) 2848–2853, https://doi.org/10.1073/pnas.161157611.
[4] M.B. Perez, V.M. Lipinski, M.F. Fillipini, K. Chacon Madrid, M.A.Z. Arruda, R. G. Wuilloud, Distribution, accumulation and speciation of selenium at the different growth stages of four garlic clones, Food Addit. Contam. Part A 38 (2021) 1506–1519, https://doi.org/10.1080/19440049.2021.1933206.
[5] V. García Márquez, Á. Morelos Moreno, A. Benavides Mendoza, J. Medrano Macías, Ionic selenium and nanoselenium as biofortifiers and stimulators of plant metabolism, Agronomy 10 (2020) 1399, https://doi.org/10.3390/agronomy10091399.
[6] P.A. Counce, T.C. Keisling, A.J. Mitchell, A uniform, objective, and adaptive system for expressing rice development, Crop Sci. 40 (2000) 436–443, https://doi.org/10.2135/cropsci2000.402436x.
[7] F.C. Lidon, K. Oliveira, M.M. Ribeiro, J. Pelica, I. Pataco, J.C. Ramalho, A.D. Leitão, A.S. Almeida, P.S. Campos, A.I. Ribeiro-Barros, I.P. Pais, M.M. Silva, M.F. Pessoa, F. H. Reboredo, Selenium biofortification of rice grains and implications on macronutrients quality, J. Cereal. Sci. 81 (2018) 22–29, https://doi.org/10.1016/j.jcs.2018.03.010.
[8] Y.D. Wang, X. Wang, Y.S. Wong, Generation of selenium-enriched rice with enhanced grain yield, selenium content and bioavailability through fertilisation with selenite, Food Chem. 141 (2013) 2385–2393, https://doi.org/10.1016/j.foodchem.2013.05.095.
[9] D.C. Freitas, A.M. de Andrade, L.F. da Costa, R.A. Azevedo, M.A.Z. Arruda, There is plenty of room at the plant science: a review of nanoparticles applied to plant cultures, Ann. Appl. Biol. 178 (2021) 149–168, https://doi.org/10.1111/aab.12640.
[10] J. Wojcieszek, J. Jiménez-Lamana, L. Ruzik, J. Szpunar, M. Jarosz, To-do and not-to-do in model studies of the uptake, fate and metabolism of metal-containing nanoparticles in plants, Nanomaterials 10 (2020) 1480, https://doi.org/10.3390/nano10081480.
[11] G. Moreno-Martín, J. Sanz-Landaluze, M.E. León-González, Y. Madrid, Insights into the accumulation and transformation of Ch-SeNPs by Raphanus sativus and Brassica juncea: effect on essential elements uptake, Sci. Total Environ. 725 (2020) 138453, https://doi.org/10.1016/j.scitotenv.2020.138453.
[12] Q. Wang, Y. Yu, J. Li, Y. Wan, Q. Huang, Y. Guo, H. Li, Effects of different forms of selenium fertilizers on Se accumulation, distribution, and residual effect in winter wheat–summer maize rotation system, J. Agric. Food Chem. 65 (2017) 1116–1123, https://doi.org/10.1021/acs.jafc.6b05149.
[13] Y. Wang, L.J. Feng, X.D. Sun, M. Zhang, J.L. Duan, F. Xiao, Y. Lin, F.P. Zhu, X. P. Kong, Z. Ding, X.Z. Yuan, Incorporation of selenium derived from nanoparticles into plant proteins in vivo, ACS Nano 17 (2023) 15847–15856, https://doi.org/10.1021/acsnano.3c03739.
[14] H.R. El-Ramady, É. Domokos-Szabolcsy, N.A. Abdalla, T.A. Alshaal, T.A. Shalaby, A. Sztrik, J. Prokisch, M. Fári, Selenium and nano-selenium in agroecosystems, Environ. Chem. Lett. 12 (2014) 495–510, https://doi.org/10.1007/s10311-014-0476-0.
[15] B.M. Freire, C.N. Lange, Y.T. Cavalcanti, L.R. Monteiro, J.C. Pieretti, A.B. Seabra, B.L. Batista, The dual effect of Selenium nanoparticles in rice seedlings: from increasing antioxidant activity to inducing oxidative stress, Plant Stress 11 (2024) 100372, https://doi.org/10.1016/j.stress.2024.100372.
[16] B. Hussain, Q. Lin, Y. Hamid, M. Sanaullah, L. Di, M.L.R. Hashmi, M.B. Khan, Z. He, X. Yang, Foliage application of selenium and silicon nanoparticles alleviates Cd and Pb toxicity in rice (Oryza sativa L.), Sci. Total Environ. 712 (2020) 136497, https://doi.org/10.1016/j.scitotenv.2020.136497.
[17] C. Wang, T. Cheng, H. Liu, F. Zhou, J. Zhang, M. Zhang, X. Liu, W. Shi, T. Cao, Nano-selenium controlled cadmium accumulation and improved photosynthesis in indica rice cultivated in lead and cadmium combined paddy soils, J. Environ. Sci. 103 (2021) 336–346, https://doi.org/10.1016/j.jes.2020.11.005.
[18] D. Bao, Z.G. Oh, Z. Chen, Characterization of silver nanoparticles internalized by Arabidopsis plants using single particle ICP-MS analysis, Front. Plant Sci. 7 (2016) 32, https://doi.org/10.3389/fpls.2016.00032.
[19] D. Mozhayeva, C. Engelhard, A critical review of single particle inductively coupled plasma mass spectrometry–A step towards an ideal method for nanomaterial characterization, J. Anal. At. Spectrom. 35 (2020) 1740–1783, https://doi.org/10.1039/C9JA00206E.
[20] M. Resano, M. Aramendía, E. García-Ruiz, A. Bazo, E. Bolea-Fernandez, F. Vanhaecke, Living in a transient world: ICP-MS reinvented via time-resolved analysis for monitoring single events, Chem. Sci. 13 (2022) 4436–4473, https://doi.org/10.1039/D1SC05452J.
[21] B.M. Freire, Y.T. Cavalcanti, C.N. Lange, J.C. Pieretti, R.M. Pereira, M. C. Gonçalves, G. Nakazato, A.B. Seabra, B.L. Batista, Evaluation of collision/reaction gases in single-particle ICP-MS for sizing selenium nanoparticles and assessment of their antibacterial activity, Nanotechnol 33 (2022) 355702, https://doi.org/10.1088/1361-6528/ac723e.
[22] J. Verstegen, K. Günther, Biosynthesis of nano selenium in plants, Artif. Cells, Nanomed. Biotechnol. 51 (2023) 13–21, https://doi.org/10.1080/21691401.2022.2155660.
[23] J. Sucharová, Optimisation of DRC ICP-MS for determining selenium in plants, J. Anal. At. Spectrom. 26 (2011) 1756–1762, https://doi.org/10.1039/C1JA10095E.
[24] E. Bolea-Fernandez, D. Leite, A. Rua-Ibarz, T. Liu, G. Woods, M. Aramendia, M. Resano, F. Vanhaecke, On the effect of using collision/reaction cell (CRC) technology in single-particle ICP-mass spectrometry (SP-ICP-MS), Anal. Chim. Acta 1077 (2019) 95–106, https://doi.org/10.1016/j.aca.2019.05.077.
[25] J. Nath, I. Dror, P. Landa, T. Vanek, I. Kaplan-Ashiri, B. Berkowitz, Synthesis and characterization of isotopically-labeled silver, copper and zinc oxide nanoparticles for tracing studies in plants, Environ. Pollut. 242 (2018) 1827–1837, https://doi.org/10.1016/j.envpol.2018.07.084.
[26] A. Laycock, B. Stolpe, I. Römer, A. Dybowska, E. Valsami-Jones, J.R. Lead, M. Rehkämper, Synthesis and characterization of isotopically labeled silver nanoparticles for tracing studies, Environ. Sci.: Nano 1 (2014) 271–283, https://doi.org/10.1039/C3EN00100H.
[27] J. Jiménez-Lamana, J. Wojcieszek, M. Jakubiak, M. Asztemborska, J. Szpunar, Single particle ICP-MS characterization of platinum nanoparticles uptake and bioaccumulation by Lepidium sativum and Sinapis alba plants, J. Anal. At. Spectrom. 31 (2016) 2321–2329, https://doi.org/10.1039/C6JA00201C.
[28] E. Sales, E. Miedes, L. Marqués, Breeding for low temperature germinability in temperate japonica rice varieties: analysis of candidate genes in associated QTLs, Agronomy 11 (2021) 2125, https://doi.org/10.3390/agronomy11112125.
[29] H.E. Pace, N.J. Rogers, C. Jarolimek, V.A. Coleman, C.P. Higgins, J.F. Ranville, Determining transport efficiency for the purpose of counting and sizing nanoparticles via single particle inductively coupled plasma mass spectrometry, Anal. Chem. 83 (2011) 9361–9369, https://doi.org/10.1021/ac201952t.
[30] E. Bolea-Fernandez, D. Leite, A. Rua-Ibarz, L. Balcaen, M. Aramendía, M. Resano, F. Vanhaecke, Characterization of SiO2 nanoparticles by single particle-inductively coupled plasma-tandem mass spectrometry (SP-ICP-MS/MS), J. Anal. At. Spectrom. 32 (2017) 2140–2152, https://doi.org/10.1039/C7JA00138J.
[31] R. Peters, Z. Herrera-Rivera, A. Undas, M. van der Lee, H. Marvin, H. Bouwmeester, S. Weigel, Single particle ICP-MS combined with a data evaluation tool as a routine technique for the analysis of nanoparticles in complex matrices, J. Anal. At. Spectrom. 30 (2015) 1274–1285, https://doi.org/10.1039/C4JA00357H.
[32] S. Boroumand, M. Safari, E. Shaabani, M. Shirzad, R. Faridi-Majidi, Selenium nanoparticles: synthesis, characterization and study of their cytotoxicity, antioxidant and antibacterial activity, Mater. Res. Express 6 (2019) 0850d8, https://doi.org/10.1088/2053-1591/ab2558.
[33] B. Gammelgaard, S. Stürup, M.V. Christensen, Human urinary excretion and metabolism of 82Se-enriched selenite and selenate determined by LC-ICP-MS, Metallomics 4 (2012) 149–155, https://doi.org/10.1039/c2mt00163b.
[34] P. Van Dael, J. Lewis, D. Barclay, Stable isotope-enriched selenite and selenate tracers for human metabolic studies: a fast and accurate method for their preparation from elemental selenium and their identification and quantification using hydride generation atomic absorption spectrometry, J. Trace Elem. Med. Biol. 18 (2004) 75–80, https://doi.org/10.1016/j.jtemb.2004.04.005.
[35] F. Laborda, A.C. Gimenez-Ingalaturre, E. Bolea, J.R. Castillo, About detectability and limits of detection in single particle inductively coupled plasma mass

spectrometry, Spectrochim. Acta B: At. Spectrosc. 169 (2020) 105883, https://doi.org/10.1016/j.sab.2020.105883.
[36] F. Laborda, E. Bolea, J. Jimenez-Lamana, Single particle inductively coupled plasma mass spectrometry: a powerful tool for nanoanalysis, Anal. Chem. 86 (2014) 2270–2278, https://doi.org/10.1021/ac402980q.
[37] F.P. Paniz, T. Pedron, V.A. Procópio, C.N. Lange, B.M. Freire, B.L. Batista, Selenium biofortification enhanced grain yield and alleviated the risk of arsenic and cadmium toxicity in rice for human consumption, Toxics 11 (2023) 362, https://doi.org/10.3390/toxics11040362.
[38] M.U. Farooq, Z. Tang, R. Zeng, Y. Liang, Y. Zhang, T. Zheng, H.H. Ei, X. Ye, X. Jia, J. Zhu, Accumulation, mobilization, and transformation of selenium in rice grain provided with foliar sodium selenite, J. Sci. Food Agric. 99 (2019) 2892–2900, https://doi.org/10.1002/jsfa.9502.
[39] S.M. Joshi, S. De Britto, S. Jogaiah, S.I. Ito, Mycogenic selenium nanoparticles as potential new generation broad spectrum antifungal molecules, Biomolecules 9 (2019) 419, https://doi.org/10.3390/biom9090419.
[40] V. Kantorová, G. Krausová, I. Hyršlová, M. Loula, O. Mestek, A. Kaňa, Determination of selenium nanoparticles in fermented dairy products, Spectrochim. Acta B: At. Spectrosc. 199 (2023) 106592, https://doi.org/10.1016/j.sab.2022.106592.
[41] Z.H. Lin, C.R.C. Wang, Evidence on the size-dependent absorption spectral evolution of selenium nanoparticles, Mater. Chem. Phys. 92 (2005) 591–594, https://doi.org/10.1016/j.matchemphys.2005.02.023.
[42] K. Wang, Y. Wang, K. Li, Y. Wan, Q. Wang, Z. Zhuang, Y. Guo, H. Li, Uptake, translocation and biotransformation of selenium nanoparticles in rice seedlings (Oryza sativa L.), J. Nanobiotechnol. 18 (2020) 1–15, https://doi.org/10.1186/s12951-020-00659-6.
[43] N. Hadrup, G. Ravn-Haren, Toxicity of repeated oral intake of organic selenium, inorganic selenium, and selenium nanoparticles: a review, J. Trace Elem. Med. Biol. 79 (2023) 127235, https://doi.org/10.1016/j.jtemb.2023.127235.
[44] A. Kumar, K.S. Prasad, Role of nano-selenium in health and environment, J. Biotechnol. 325 (2020) 152, https://doi.org/10.1016/j.jbiotec.2020.11.004.
[45] H. El-Ramady, S.E.-D. Faizy, N. Abdalla, H. Taha, E. Domokos-Szabolcsy, M. Fari, T. Elsakhawy, A.E.-D. Omara, T. Shalaby, Y. Bayoumi, S. Shehata, C.-M. Geilfus, E. C. Brevik, Selenium and nano-selenium biofortification for human health: opportunities and challenges, Soil Syst 4 (2020) 57, https://doi.org/10.3390/soilsystems4030057.
[46] N. Hadrup, G. Ravn-Haren, Absorption, distribution, metabolism and excretion (ADME) of oral selenium from organic and inorganic sources: a review, J. Trace Elem. Med. Biol. 67 (2021) 126801, https://doi.org/10.1016/j.jtemb.2021.126801.
[47] B.M. Freire, V. da Silva Santos, P.C.F. Neves, J.M.O.S. Reis, S.S. de Souza, F. Barbosa Jr, B.L. Batista, Elemental chemical composition and as speciation in rice varieties selected for biofortification, Anal. Methods 12 (2020) 2102–2113, https://doi.org/10.1039/D0AY00294A.
[48] R. Batista, M. Oliveira, Plant natural variability may affect safety assessment data, Regul. Toxicol. Pharmacol. 58 (2010) S8–S12, https://doi.org/10.1016/j.yrtph.2010.08.019.
[49] A.B.S. da Silva, M.A.Z. Arruda, Exploring single-particle ICP-MS as an important tool for the characterization and quantification of silver nanoparticles in a soybean cell culture, Spectrochim. Acta B: At. Spectrosc. 203 (2023) 106663, https://doi.org/10.1016/j.sab.2023.106663.
[50] Y. Huang, J.T. Lum, K.S. Leung, Single particle ICP-MS combined with internal standardization for accurate characterization of polydisperse nanoparticles in complex matrices, J. Anal. At. Spectrom. 35 (2020) 2148–2155, https://doi.org/10.1039/d0ja00180e.
[51] M. Aramendía, J.C. García-Mesa, E.V. Alonso, R. Garde, A. Bazo, J. Resano, M. Resano, A novel approach for adapting the standard addition method to single particle-ICP-MS for the accurate determination of NP size and number concentration in complex matrices, Anal. Chim. Acta 1205 (2022) 339738, https://doi.org/10.1016/j.aca.2022.339738.
[52] N. Srivastava, M. Mukhopadhyay, Green synthesis and structural characterization of selenium nanoparticles and assessment of their antimicrobial property, Bioprocess, Biosyst. Eng. 38 (2015) 1723–1730, https://doi.org/10.1007/s00449-015-1413-8.
[53] M. Murali, H.G. Gowtham, S. Brijesh Singh, N. Shilpa, M. Aiyaz, M.N. Alomary, M. Alshamrani, A. Salawi, Y. Almoshari, M.A. Ansari, K.N. Amruthesh, Fate, bioaccumulation and toxicity of engineered nanomaterials in plants: current challenges and future prospects, Sci. Total Environ. 811 (2022) 152249, https://doi.org/10.1016/j.scitotenv.2021.152249.
[54] S. Adhikari, A. Adhikari, S. Ghosh, D. Roy, I. Azahar, D. Basuli, Z. Hossain, Assessment of ZnO-NPs toxicity in maize: an integrative microRNAomic approach, Chemosphere 249 (2020) 126197, https://doi.org/10.1016/j.chemosphere.2020.126197.
[55] L.A. Paramo, A.A. Feregrino-Pérez, R. Guevara, S. Mendoza, K. Esquivel, Nanoparticles in agroindustry: applications, toxicity, challenges, and trends, Nanomaterials 10 (2020) 1654, https://doi.org/10.3390/nano10091654.
[56] E. Kabir, V. Kumar, K.H. Kim, A.C. Yip, J.R. Sohn, Environmental impacts of nanomaterials, J. Environ. Manage. 225 (2018) 261–271, https://doi.org/10.1016/j.jenvman.2018.07.087.